

PRELIMINARY NOTES

An Efficient, Gaseous Detector with Good Low-energy Resolution for (≤ 50 keV) Imaging

Nguyen Ngoc Hoan, S. Majewski, G. Charpak, and A.J.P.L. Policarpo

*Institut National de Physique Nucléaire et de Physique des Particules, Accélérateur linéaire,
Orsay, France,
University of Warsaw, Warsaw, Poland, and University of Coimbra, Coimbra, Portugal*

An imaging detector with good energy resolution and reasonable spatial accuracy has been designed for biomedical applications. It is based on a scintillating proportional gas chamber. The energy resolution is typically 5.4% (FWHM) at 27 keV and the spatial resolution is 2.7 mm (FWHM) for 22-keV x-rays. The physical processes involved in this detector are discussed along with its main limitations and merits.

J Nucl Med 20: 335-340, 1979

Most of the instruments used for determination of the spatial distribution of gamma photons are at present based on the location of the conversion points in scintillators, usually NaI crystals (1).

Multiwire proportional chambers and drift chambers of various geometries are being actively investigated as alternative detectors (2,3). They are finding prospective applications mostly in fields where low-energy photons (< 100 keV) are required and where high-pressure gaseous filling, consisting mainly of xenon, should provide acceptable efficiency.

Some of the properties of these detectors are advantageous compared with the scintillation camera: better spatial accuracy, good energy resolution below ~ 50 keV, and much higher rate capability.

Some examples of applications making use of these specific properties have recently been reported—for instance, in the measurement of the mineral content in bones, where sources of 42-keV x-rays emitted by Gd-153 are well suited to absorptiometry measurements (4,5). Moreover, this energy range is well suited to small-animal imaging, either with radionuclides or with fluorescence induced by x-rays.

The scintillation proportional chamber (6), a newcomer among gaseous detectors, offers substantial advantages over wire-type proportional chambers. In the former, two main regions are considered. In the first—the detection, conversion, or drift region—the radiation is absorbed, ion pairs are produced, and the electrons are drifted in a region of low electric field such that recombination effects are absent and there is no excitation of the medium. The type of interaction associated with the detection of the radiation and the statistics of ion-pair production are determined by the properties of the radiation and the detecting medium.

The electrons drift toward a second region—the so-called light-emitting or secondary light-production space—where there is a strong electric field such that the drift of the electrons in the region gives rise to excitation of the medium but not to its ionization.

The properties mainly responsible for the favorable spatial and energy resolutions of this system, together with its tolerance of high counting rates, are the generous light output derived from the de-excitation of the medium, the absence of charge multiplication, and the emission of light from the drift of the electrons in only a small region (typically a few millimeters) whose dimensions are controllable simply by the configuration of the electric field.

Received May 15, 1978; revision accepted Nov. 1, 1978.

For reprints contact: Nguyen Ngoc Hoan, Laboratoire de l'Accelerateur Linéaire, Centre d'Orsay, Orsay 91405, France.

To take full advantage of the intrinsic properties of the gas-scintillation proportional counter, the gas must be pure and the system clean (impurities are strong quenchers of its light emission), and one must provide for good light transmission out of the chamber to the light-detecting devices, usually photomultipliers.

When the energetic electrons drift into the light-emitting space, they excite the gas atoms along their paths and ultraviolet photons are emitted following the decay of the dimers associated with the de-excitation of those atoms. In general the uv light is emitted in a range of wavelengths too far from the region of good sensitivity of the photomultipliers to be detected efficiently. So, either one uses a window that is transparent to the far uv range (Ca F_2 , Mg F_2 , LiF , etc.) and a suitable wavelength shifter is deposited on the external surface of the window; or a wavelength shifter is deposited on the inside of the container, in contact with the gas, and the container wall must transmit the re-emitted light. Large-diameter windows transparent to the far uv are very expensive, so the latter solution is generally adopted. Of course, this solution has the disadvantage that the layer of the wavelength shifter is a source of impurities that poison the pure gas and reduce its light output. The filling gas can be continuously purified by circulating it through a suitable purifier, for example, calcium turnings at about 400°C.

The properties of these detectors that have aroused considerable interest for some applications are the following.

1. The amount of light that can be collected after absorption of ionizing radiation is about 100 times greater, per keV deposited, than with a NaI scintillator (6).

2. The energy resolution is much better than with any other proportional chamber. At 6 keV, resolutions of 8.5% (FWHM) are obtained (6-8). In general the energy resolution is about a factor of two better than with wire chambers.

3. Only the solid-state detectors are superior in energy resolution, but they do not permit large surfaces of detection at low cost.

4. The counting rate is not limited by any space-charge effect characteristic of amplification around wires, and rates of 3 million/sec per mm^2 have been reported, without saturation effects (9).

5. Pure xenon or other noble gases are being used without the addition of quenching agents. These agents, which are essential in high-gain wire chambers, are decomposed by the amplification process and their renewal is difficult with a gas-tight sealed detector.

We report here a study concerning applications where good energy and spatial resolutions are needed together with relatively high counting rates and reasonable detection efficiencies. The filling gas was xenon at 1 atm.

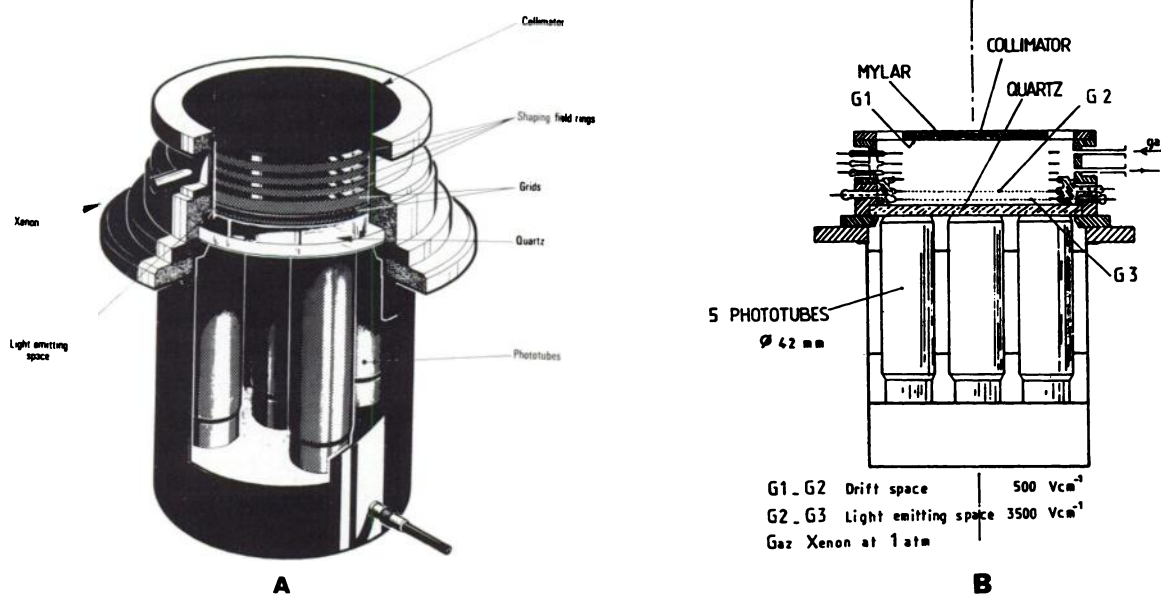


FIG. 1. (A) Detector of energy-sensitive x-ray camera using gas scintillator. (B) Photons absorbed in xenon in drift space produce photoelectrons that drift into light-producing space. Ultraviolet light is converted into visible light by wavelength shifter deposited on quartz window. Five photomultipliers view the scintillations. On-line computing based on microprocessor gives position of centroid of spatial position of light-emitting track.

A SCINTILLATION PROPORTIONAL COUNTER WITH IMAGING PROPERTIES

Experimental system and main functions. Figure 1A shows the arrangement of the chamber and photomultiplier assembly, and a cutaway drawing is shown in Fig. 1B. The useful diameter of the window is 110 mm. The drift space, where the incident x-rays interact and the dislodged electrons drift without excitation, lies between the grids G_1 and G_2 , a distance of 50 mm. This is the low-field region, typically about 500 V/cm. Grids G_2 and G_3 define the light-emitting space, 6 mm thick, where the electron drift gives rise to light emission without charge multiplication. Typical fields used were ~ 3.5 kV/cm. Another region, lying between grid G_3 and the quartz window, a distance of 16 mm, is simply an electron trap; although most of the electrons in the gap $G_2 - G_3$ are collected by G_3 , some may leak through, and these could, if no space were present, impinge on the quartz window producing luminescence and building up a charge. The optical transparency of each grid used is $\sim 90\%$.

This structure is viewed by an assembly of five photomultipliers (EMI 9750 QR), 2 in. in diameter, through a quartz window whose inside surface is covered with a layer of p-terphenyl 1 mg/cm² thick (10). It is deposited by vacuum evaporation, with continuous rotation of the quartz disc to encourage uniform deposition. The uv light from the xenon scintillations has wavelengths in the 150-to-190 nm range (8), but the p-terphenyl re-emits at around 350 nm, a wavelength for which the phototubes provide good sensitivity. Moreover, the quartz windows of the chamber and the phototubes are highly transparent to this radiation. Good efficiency of light transmission to the outside of the chamber—essential for both energy and spatial resolution is thus obtained, but the need for continuous purification arises. The purifier is simply a vertical stainless steel cylinder, containing about 300 g of metallic calcium and heated to about 400°C. It is directly connected at top and bottom to an inlet and an outlet on the gas chamber, and the convection current eliminates the need for forced circulation. Initially, the system is pumped down to 10^{-4} torr during several hours, with the calcium purifier kept at about 600°C, to clean up the chamber. The temperature is then reduced to 440° and one atm of xenon is let in. During the first three hours there is a continuous improvement in light output and resolution, but the detector remains very stable thereafter. The system has been tested and has remained stable over 4 months of continuous operation.

The five photomultipliers are disposed in an array with one at the center and the other four symmetrically distributed around it, forming a square

whose diagonal is 12 cm. This is by no means an ideal arrangement for the provision of energy and spatial resolution, which demand many samplings and minimum light loss. (Currently only half of the light coming through the quartz window is put to use.) Ideally there should be many photomultipliers, such that the centroid of the sampling signals corresponds as nearly as possible to the X and Y coordinates of the interaction point.

Although the pulses from the phototubes could be handled better by standard gamma-camera electronics from the point of view of data storage and processing, we have used a low-cost microprocessor-based version, tolerating the decreased counting-rate performance for on-line processing.

Full use should be made of the total light output, and a good measurement calls for signal integration during a time at least equal to the duration of the light signal. Since light is emitted during the electron drift in the light-emitting space, the drift velocity of about 2 μ sec/cm (which occurs in xenon at 1 atm with a field of 3.5 kV/cm) implies an integration time of 1.2 μ sec. Another effect, diffusion of the initial electron cluster during its drift through the detection region, intensifies the light signal. An integration time of 2 μ sec was therefore used in the experiments reported. This process imposes an intrinsic counting-rate limitation on the particular detector used, a function of its geometry, the applied voltages, and the nature of the contained gas.

EXPERIMENTAL RESULTS AND DISCUSSION

Spatial resolution and linearity. If reasonable parameters are taken for the light output from the chamber, its spatial distribution as affected by the wavelength-shifter, and the resolutions of the photomultipliers, one would expect that an energy deposition of about 15 keV at a point would yield a FWHM spatial resolution of about 2.5 mm. This gives an indication of the intrinsic capabilities of the device. Careful attention should be given, however, to the several steps in the interaction of the x-ray with the detecting medium, particularly how well localized the x-ray energy deposition in it will be. No details will be considered here, since a complete analysis of this process has been made by J. E. Bateman et al. (11), for xenon filling and for the range of x-ray energies for which the chamber under study has useful efficiencies. For particular lengths associated with x-ray emission from the interacting atoms set limits on the spatial resolution that have nothing to do with the intrinsic spatial resolution of the chamber; they are a natural limit in any gaseous device.

Based on these initial considerations, we can report now the experimental results. Referring to Fig.

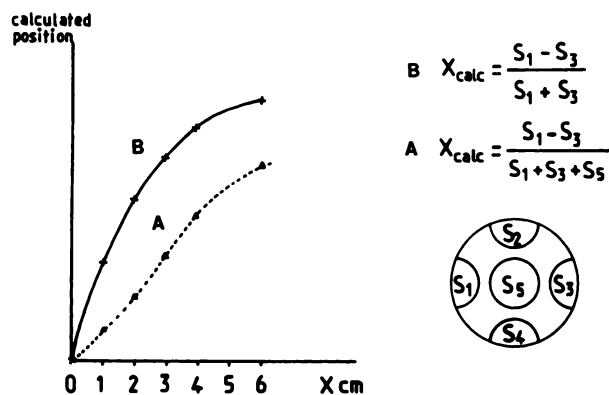


FIG. 2. Spatial linearity measured with collimated Cd-109 source along line joining centers of photomultipliers, S_1 and S_3 .

2, the coordinates x and y were derived from weighted differences of signals S_i from diametrically situated photomultipliers:

$$x = \frac{S_1 - S_3}{S_1 + S_3 + S_5}; \quad y = \frac{S_2 - S_4}{S_2 + S_4 + S_5}.$$

Curve A of Fig. 2 plots the real position against the chamber reading for x , determined by moving a collimated beam of x-rays (~ 22 keV) from a Cd-109 source along the X axis. The nonlinearity is less than 10%, except near the edge region—as one would expect owing to the effect of the chamber wall and the simplified expressions used for X and Y . The simpler approximations usually used— $X = S_1 - S_3/S_1 + S_3$ and $Y = S_2 - S_4/S_2 + S_4$ —give good linearity only for events close to the center, as can be seen from curve B of Fig. 2. It is clear that without increasing the chamber size, the use of information from the center photomultiplier improves the overall linearity of the chamber.

The spatial resolution was tested with an x-ray generator, operating at 25 kV and filtered with 20 μm of copper foil, placed 20 cm above a lead mask containing a set of five holes disposed in a line at regular intervals. The line of holes coincides with the X direction (Fig. 2), the first hole being placed at the chamber center and the direction defined by the third hole. The x-ray source is parallel to the electric field in the chamber. Figure 3A shows the display obtained from holes 1 mm in diameter and spaced 10 mm apart. The corresponding intensity distribution along the central line of these holes is shown in Fig. 3B. A resolution of 2.7 mm (FWHM) is obtained even for the second hole, including all effects such as hole size, parallax, finite source-to-mask distance and finite source size (~ 1 mm). The parallax effect is clearly observable in both Figs. 3A and B.

Energy resolution, linearity, and spatial uniformity. The detailed physical tests of the detector's energy resolution and energy linearity have been reported elsewhere (12). We summarize the main features here. The energy linearity and resolution of the system are shown in Fig. 4A, where the several x-ray energies are derived either from radioactive sources or from fluorescence induced by the 60-keV x-rays from Am-241. The energy resolution, which is $\sim 5.4\%$ (FWHM) at 30 keV, varies as $(1 + 22/\sqrt{E} \text{ (keV)})\%$, an expression that simply summarizes the experimental data obtained. The energy resolution of the detector for x-rays of biologic interest is shown in Fig. 4B.

The response uniformity in terms of signal amplitudes as well as energy resolution was experimentally measured and is shown in Fig. 5. The signal amplitudes are normalized to one at the center of the chamber and the energy resolutions corresponding to a value of 6%, also at the center. Several effects account for the nonuniformity seen, wall effects of course, but also the nonuniformity

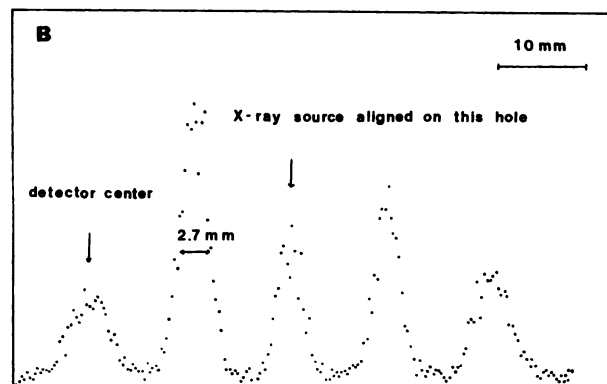
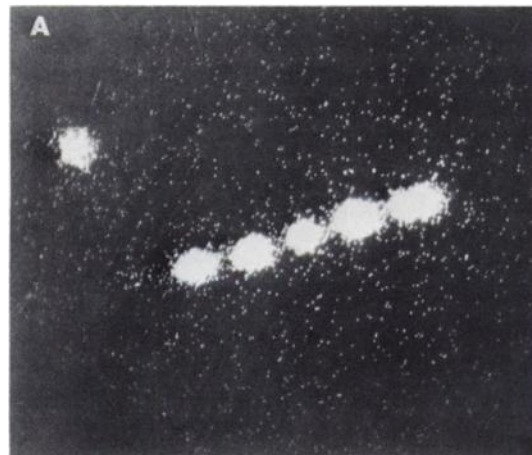


FIG. 3. Spatial resolution: holes 1 mm in diameter, 10 mm apart, in a lead mask; x-ray generator at 25 keV, 20 cm above mask. (A) Image obtained in 2 min. (B) Projection along line of holes showing spatial resolution of 2.7 mm (FWHM) at second hole.

in the thickness of the p-terpheryl layer and the small number of photomultipliers used.

Sensitivity and counting rate. As mentioned earlier, the light pulses were integrated over 2 μ sec, and this sets the intrinsic counting-rate limitation of the chamber. A rate of about 10^5 events per second should not spoil the characteristics of the detector considered in Sections A and B of this discussion. The overall background rate arising from noise, cosmic rays and, microdischarges in the gas is of the order of 1 count/min-cm² for a rather broad energy window to account for the amplitude reduc-

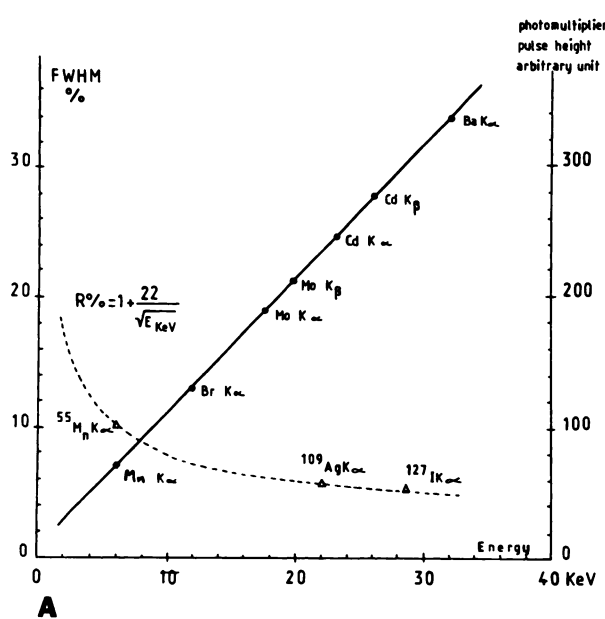


FIG. 4. (A) Energy resolution and linearity of detector observed with radioactive sources and fluorescence spectra induced by 60-keV radiation from Am-241. (B) Energy resolution of camera. Spectrum of x-rays emitted at 130° relative to 60-keV beam emitted by Am-241, impinging on a 3% solution of KI in water. Shown are K α and K β lines of iodine (27.5 and 31.0 keV) with a resolution of 5.4%. Lower-energy peaks are K $_{\alpha\alpha}$, xenon escape peaks from the Compton radiation scattered at 130°.

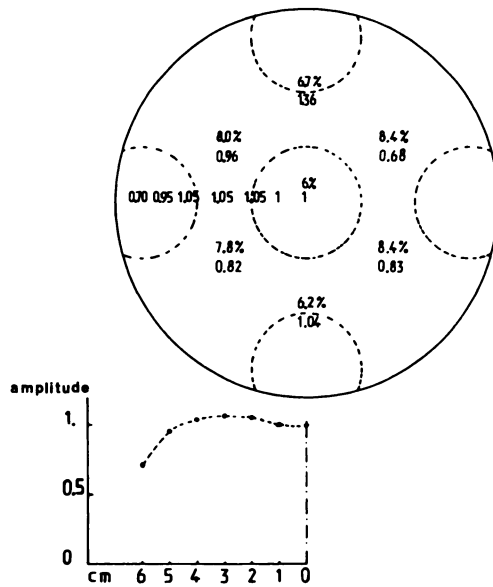


FIG. 5. Spatial response uniformity. Pulse amplitude vs distance along X direction, measured with Ag x-rays (22 keV) from Cd-109 source.

tion at the edge of the detector. Depending on the required contrast, this figure allows for the sensitivity determination.

Imaging properties. The quality of the detector has been tested with phantoms and animals. A thyroid phantom filled with 30 μ Ci of I-125 and placed against a multihole silver collimator gives a good image including proper display of the 4-mm hypoactive region (Fig. 6).

Figure 7 shows a thyroid image obtained in 2 min from an unanesthetized rabbit, 24 hr after injection of 100 μ Ci of I-125. This image was obtained with this instrument in a program of research on animals currently in progress at the Faculte de Medecine Bordeaux II.

CONCLUSION

Our results show that among detectors, the scintillating proportional counter is quite appropriate for imaging purposes similar to those used with solid scintillators. It is at present the best detector for applications where good energy resolution combined with a large surface is required in the x-ray energy range around or below 50 keV. For higher energies, higher pressures are required for reasons of both efficiency and spatial accuracy.

Throughout this paper we have pointed out that the conditions we used were far from optimal considering the intrinsic capabilities of the device. Probably the main handicap was that about half of the light transmitted through the quartz window of

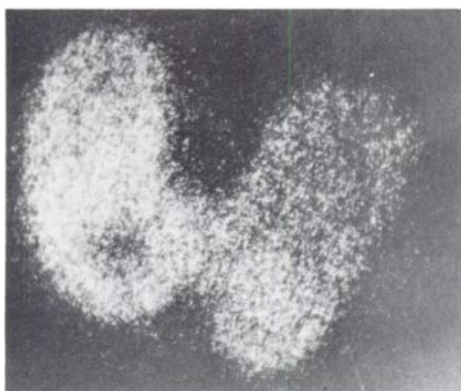


FIG. 6. Image of thyroid phantom (Picker No. 3602) filled with $30 \mu\text{Ci}$ of I-125. Collimator has 1-mm holes, septa 0.1 mm, length 20 mm, transmission 1.24×10^{-4} . Acquisition time 3 min.

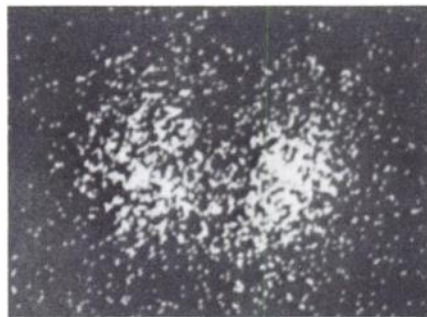


FIG. 7. Thyroid image from unanesthetized rabbit with $100 \mu\text{Ci}$ of I-125 injected 24 hr before observation. Acquisition time 2 min.

the chamber was lost, mainly because of the small number of photomultipliers used. Both energy and spatial resolutions, as well as uniformity of response, were thus constrained. Moreover, the counting-rate efficiency was less than optimal, since a decrease in the thickness of the light-emitting space could improve the maximum counting rate that can be handled usefully.

The chamber is versatile in the sense that other and cheaper scintillators could be used, such as krypton. Work at high pressures will provide for an increase of detection efficiency, and if one permitted a small charge multiplication with proper electronic circuitry, an improvement of the spatial re-

solution of the device could be achieved, with no loss of energy resolution or rate performance.

We are continuing our investigations in these directions. Preliminary measurements show that detectors applying this principle at high pressure could be useful tools in various fields.

ACKNOWLEDGMENTS

This investigation has been made possible by a grant from the Délégation Générale à la Recherche Scientifique et Technique. We are grateful to Professor J. Yoccoz for his continual interest and support from IN2P3. Thanks are due also to Professor Kellersohn for providing us with a collimator and radioactive phantoms. One of us (NNH) is particularly indebted to Professor J. Perez-Y-Jorba for his constant encouragement and support. Another author (AJPLP) acknowledges a leave of absence from the Physics Department of the University of Coimbra, Portugal.

REFERENCES

1. FREEDMAN JS: *Tomographic Imaging in Nuclear Medicine*. New York, Society of Nuclear Medicine, 1972, pp 1-40
2. PEREZ-MENDEZ V: Proportional and drift chamber in applied investigations. Lawrence Berkeley Laboratory report no. 3851, 1975
3. CHARPAK G: Applications of proportional chambers to some problems in medicine and biology: Wire chamber conference, Vienna, 1978. *Nucl Instr Meth* 156: 1-17, 1978
4. HORSMAN A, READING DH, CONNOLLY J, et al: Bone imaging using a gadolinium-153 source and xenon-filled multiwire proportional counter as detector. *Amer J Roentgenol* 126: 1273-1275, 1976
5. ZIMMERMAN RE, LANZA RC, TANAKA T, et al: A new detector for absorptiometric measurement. *Amer J Roentgenol* 126: 1272-1273, 1976
6. POLICARPO AJPL, ALVES MA, DOS SANTOS MCM, et al: Improved resolution for low energies with gas proportional scintillation counters. *Nucl Instr Meth* 102: 337-348, 1972
7. PALMER HE, BRABY LA: A parallel plate gas scintillating proportional counter for improved resolution of low-energy photons. *Nucl Instr Meth* 116: 587-589, 1974
8. ANDERSEN RD, LEIMANN EA, PEACOCK A, et al: Recent progress in the development of gas scintillating proportional counter for X-ray astronomy. IEEE. *Trans Nucl Sci* NS 24: 810-816, 1977
9. CHARPAK G, MAJEWSKI S, SAULI F: The scintillating drift chamber: A new tool for high accuracy, very high rate particle localisation. *Nucl Instr Meth* 126: 381-389, 1975
10. POLICARPO AJPL, ALVES MAF, SALETE M, et al: Detection of soft X-rays with a xenon-scintillating proportional counter. *Nucl Instr Meth* 118: 221-226, 1974
11. BATEMAN JE, WATERS MW: An investigation of the possible application of bidimensional MWPC to X-ray absorptiometry. Rutherford Report RL 76-067, 1976
12. NGUYEN NGOC HOAN: Performances of an X-ray imaging gas scintillating proportional counter. *Nucl Instr Meth* 154: 597-601, 1978